Aligned carbon nanotubes with built-in FeN_4 active sites for electrocatalytic reduction of oxygen†

Junbing Yang, Di-Jia Liu,* Nancy N. Kariuki and Lin X. Chen

Received (in Berkeley, CA, USA) 28th August 2007, Accepted 13th November 2007
First published as an Advance Article on the web 29th November 2007
DOI: 10.1039/b713096a

The electrocatalytic site FeN_4, which is active towards the oxygen reduction reaction, is incorporated into the graphene layer of aligned carbon nanotubes prepared through a chemical vapour deposition process, as is confirmed by X-ray absorption spectroscopy and other characterization techniques.

The oxygen reduction reaction (ORR) is an important electrochemical reaction at the cathode of a polymer electrolyte membrane fuel cell (PEMFC). Oxygen combines with electrons and protons at the electrode catalyst surface to form water.[1] At present, the most effective electrode catalyst for the ORR is made of highly dispersed platinum or platinum alloys supported on carbon black. Finding an inexpensive material to replace platinum is extremely important to fuel cell cost reduction. Among many non-platinum systems being investigated, N_4 transition metal (TM)-macrocyclic compounds such as porphyrins or phthalocyanines have shown encouraging catalytic activity towards the ORR, especially after they are treated at elevated temperatures.[2,3] A series of studies by Dodelet and co-workers found that the catalysts prepared by pyrolyzing TM compounds such as iron(II) acetate supported over carbon can also achieve good ORR activity when ammonia is present during the pyrolysis.[4–7] In fact, they found that the specific nature of the precursor was not important, as long as the pyrolysis mixture contained carbon, nitrogen, and iron.[7] They attributed the ORR activity to the active sites FeN_2–C and FeN_4–C, where Fe is coordinated with two or four pyridinic or pyrrolic N atoms embedded in the conjugated carbon plane formed through iron and nitrogen doping at elevated temperature.[5,6] Recently, Ozkan and coworkers prepared N-containing nanostructured carbons and nanotubes in a vapor deposition process using acetonitrile over Fe and Ni doped alumina, Vulcan carbon and other supports. They found that these materials have promising catalytic activity towards ORR and proposed that the active site is likely located on carbon edge planes.[8,9]

We report here a method of synthesizing high purity, vertically aligned carbon nanotubes (ACNTs) with a built-in FeN_4 site through nitrogen and iron doping by a chemical vapor deposition (CVD) process. The ACNTs thus prepared were found to be catalytically active yet stable towards the ORR in an acidic electrolyte mimicking the cathode environment of PEMFC. Our structural characterization study by X-ray absorption spectroscopy revealed that the active site is composed of a divalent iron coordinated with four nitrogens in a slightly distorted square-planar configuration. The new ACNT with built-in electrocatalytic sites has unique advantages over the existing carbon black supported catalyst in the membrane electrode assembly (MEA) of the PEMFC. For example, ACNT is in a form of graphitic carbon with better resistance to oxidative corrosion. Vertically aligned nanotubes establish a direct contact between the membrane electrolyte and the current collector leading to improved thermal and electronic conductivities. By incorporating the electrochemically active site directly on the nanotube surface during ACNT growth, one could build an electrode with a three-dimensional nano-architecture and enhanced surface–gas phase interaction over the current, ink-based MEA approach.[10]

The ACNT sample was prepared by a floating catalyst CVD method[11] using ferrocene as an iron additive catalyst and ammonia as the N-dopant in a two-temperature zone reactor. The ferrocene–xylene input mixture was vaporized at the low-temperature zone and carried by an Ar–H_2 gas blend to the high-temperature zone where vertically aligned multiwalled carbon nanotubes were formed on the surface of a quartz substrate. For the reference of this study, the sample is labeled as ACNT-1 when ammonia was added in the gas blend during CVD process. To better understand the origin of the electrocatalytic activity and the active site structure, a comparative sample was also prepared under similar experimental conditions except that NH_3 was removed from the gas blend, labeled as ACNT-2. Fig. 1 shows the scanning electron microscope (SEM) images of these samples.

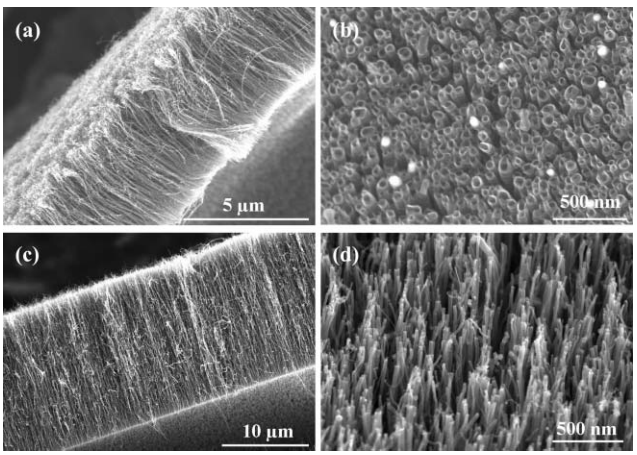

Fig. 1 SEM images of ACNTs prepared from a ferrocene–xylene blend with NH_3 (a), (b) and without NH_3 (c), (d) in the CVD input gas mixture.

Chemical Sciences & Engineering Division, Argonne National Laboratory, 9700 South Cass Ave., Argonne, IL 60439, USA. E-mail: djliu@anl.gov; Fax: +1 630-252-4176; Tel: +1 630-252-4511

† Electronic supplementary information (ESI) available: Sample preparation, electrochemical characterization, X-ray absorption data and TEM study. See DOI: 10.1039/b713096a

When ammonia is added during the CVD synthesis, nitrogen can be integrated into the graphitic plane.[12] Integration of nitrogen distorts the graphene lattice and alters the nanotubes from a straight cylinder shape, as is demonstrated through the comparison between Fig. 1(a) and (c). The competition from nitrogen also delays the carbon species from reaching the super-saturation state, thereby impeding the growth of the nanotubes. All these lead to shorter and somewhat twisted nanotubes with larger diameters than their nitrogen-free counterparts, shown in Fig. 1(b) and (d). A separate energy dispersive X-ray spectroscopy (EDS) study revealed that ACNT-1 contains an average of 3.44 at% nitrogen sampled from different regions. As expected, no nitrogen was observed in the EDS spectrum of ACNT-2.

The ACNT samples were subsequently tested in an O_2-saturated acidic electrolyte, simulating a PEMFC cathode, for ORR activity and catalyst stability. Cyclic voltammetry was used for the electrocatalytic activity measurement. A single-compartment electrochemical cell was employed, with a gold coil and Ag/AgCl (3 M NaCl) as the counter and reference electrodes, respectively. All potentials reported here have been converted to the normal hydrogen electrode reference (NHE) scale. The working electrode was prepared by coating ACNT samples on a glassy carbon surface (0.07 cm^2). To help attaching ACNTs to the electrode, a small amount of Nafion® ionomer solution (5 wt% in aliphatic alcohols, Sigma-Aldrich) was added as the binder. The ACNT electrode was soaked in the electrolyte (0.6 M $HClO_4$) for 24 h to ensure that the carbon nanotubes were completely wetted. Before the testing, the potential was cycled between 0 to 1.2 V 20 times to clean any residuals on the surface. Fig. 2 shows the cyclic voltammograms (CVs) for ACNT-1 and ACNT-2 taken in either argon- or oxygen-purged aqueous electrolyte using a potentiostat (Princeton Applied Research) at a scan rate of 10 mV s^{-1}.

A significant difference in electrocatalytic activity towards ORR was observed between the two samples. The ORR onset potential, which is determined by the potential in CV at which the electrode current in the presence of O_2 differs from the Ar-saturated background, is 0.79 V for ACNT-1. This value, however, reduced significantly to 0.40 V for ACNT-2. The electrode current also increased more rapidly with the decrease of potential for ACNT-1 in comparison with ACNT-2, as shown in Fig. 2. Clearly, the electrocatalytic activity was enhanced significantly when NH_3 was used during the CVD process. To further demonstrate the electrocatalytic activity and stability of ACNT-1, additional electrochemical measurements were performed including steady-state cyclic voltammetry, chronoamperometry, and cyclic voltammetry after the sample was treated in acidic electrolyte for extended period of time. The detailed experimental results are provided in the ESI.†

To better understand the structure of the active sites for the ORR, we conducted an X-ray absorption spectroscopy (XAS) study at the Fe K-edge at the Advanced Photon Source of Argonne National Laboratory. Both extended X-ray absorption fine structure (EXAFS) and X-ray absorption near edge structure (XANES) spectroscopic methods were used to analyze the iron coordination structure and its oxidation state inside of the ACNT. Fig. 3 shows the radial distribution functions (RDFs) for ACNT-1 and ACNT-2 obtained through Fourier transformation of k^2 weighted χ functions, extracted from the EXAFS spectra. For the electrocatalytically inactive ACNT-2, only one dominant peak was observed between 2 Å to 3 Å, which belongs to a known Fe–Fe shell. A coordination number (N) of 4.5 with an interatomic distance (R) of 2.56 Å was derived for this shell through the non-linear least-square-fitting method,[13] suggesting that iron in ACNT-2 is mainly in the form of metallic nano-crystallites. For the electrocatalytically active ACNT-1, two peaks were observed in the RDF. The peak above 2 Å also belongs to the Fe–Fe shell, as in the case of ACNT-2. The peak below 2 Å was assigned to the Fe–N shell because N-doping was the only difference between ACNT-1 and ACNT-2 and the interatomic distance falls within the range typically observed for the iron–nitrogen bond in organometallic compounds.[14] This was further confirmed by a XANES study of which the spectrum of ACNT-2 resembles highly dispersed iron metallic particles whereas the spectrum for ACNT-1 indicates a composition of at least two types of iron moieties, one of which is Fe particles in a zero-valence state (see ESI†). This observation was also corroborated by an SEM investigation, which identified the

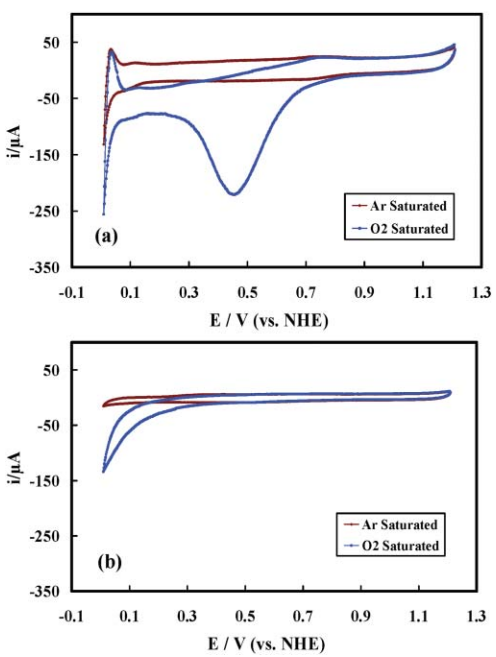

Fig. 2 CVs of ACNT-1(a) and ACNT-2 (b) measured in 0.6 M $HClO_4$ electrolyte saturated with argon or oxygen.

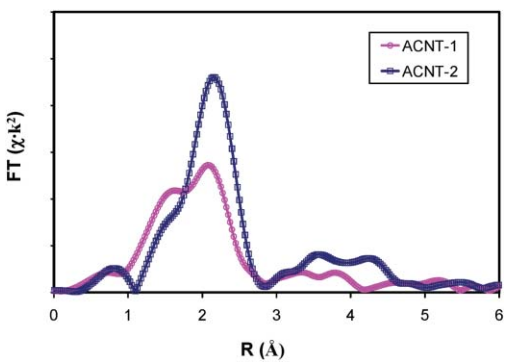

Fig. 3 The radial distribution functions of ACNTs prepared from ferrocene–xylene with ammonia (ACNT-1) and without ammonia (ACNT-2).

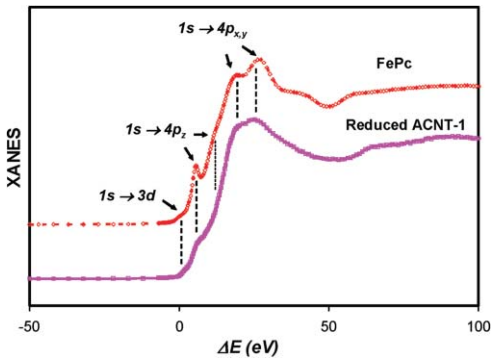

Fig. 4 Comparison of the XANES spectra of iron(II) phthalocyanine and ACNT-1 after subtraction of the metallic contribution from the spectra. $\Delta E = E - E_0$ where E is the X-ray photon energy and E_0 is Fe K-edge threshold energy.

presence of iron metal crystallites in both ACNT-1 and ACNT-2. To separate the non-metallic contribution, we removed the fraction of Fe metal crystallite from the X-ray absorption spectrum of ACNT-1 using a linear subtraction method.[13] The χ function from the reduced XAS spectrum was analyzed using the same non-linear least-square-fitting program. Iron(II) phthalocyanine (FePc) was used as the reference compound. The result showed a coordination number (N) of 4.2 and a bond length (R) of 1.95 Å of a nitrogen shell surrounding Fe. To further elucidate the structure of the second Fe component, the XANES spectrum of ACNT-1 after subtracting the metallic contribution is shown in Fig. 4, and compared with the spectrum of FePc. Among the similarities between the two near-edge spectra, the most dominant feature is the existence of several 1s → 4p transitions, which are characteristic of an iron(II) complex with square-planar configuration, a structure commonly found in four-nitrogen coordinated TM organometallic compounds.[15,16] From EXAFS and XANES analyses, we derived the structure of the electrocatalytically active site to be a ferrous ion chelated by four nitrogen atoms in a slightly distorted square-planar geometry. It is highly likely that nitrogen is in a pyridinic or a pyrrolic ring formed in the nanotube graphene plane during the high-temperature CVD process. Such types of nitrogen have been experimentally observed in N-doped carbon nanotubes prepared under similar experimental conditions through X-ray photoelectron spectroscopy.[8,17] The gaseous iron species catalyze the reaction of nitrogen with carbon during graphene sheet formation while forming the Fe–N chelating bond simultaneously. To confirm this, we examined the regions of the nanotube free of Fe metallic crystallites using transmission electron microscopy (TEM) and EDS. TEM was focused on the surface of the individual nanotube with graphitic phase in the absence of any detectable metal particles or specks. EDS clearly showed the presence of both Fe and N in these areas with N : Fe ratios ranging from 4 : 1 to 16 : 1, suggesting atomically dispersed iron embedded on to the nanotube through bonding with nitrogen.

To our knowledge, this study represents the first experimental observation of incorporating a d-metal such as Fe atomically into carbon nanotube through ligation with doped nitrogens. The observed electrocatalytic activity appears consistent with the earlier study on Fe and N-doped amorphous carbon where FeN_4–C and FeN_2–C were identified.[4,5] Inserting nitrogen in the graphene plane could cause instability interfering with nanotube growth. By coordinating with Fe, nitrogens doped at the carbon edge can form the planar FeN_4 moiety to bridge the gap and stabilize the graphene layer growth before folding into the nanotube. To verify such energy stabilization of FeN_4 in ACNT, a quantum mechanical calculation is required which is underway. We should also mention that even though FeN_4 is the predominant species, we could not preclude that a minor fraction of FeN_x (x = 1, 2 and 3) may coexist in ACNT, due to the typical uncertainty associated with EXAFS analysis in N-coordiation, which can be as high as 20%.

In summary, we have developed a versatile CVD method to prepare vertically-aligned carbon nanotube arrays electrocatalytically active toward ORR. For the first time, we identified the electrocatalytically active site in these ACNTs by X-ray absorption spectroscopic methods as a ferrous ion coordinated with four nitrogen atoms. These functionalized ACNTs show promise as an alternative non-Pt electrocatalyst with a unique nano-architecture and advantageous material properties for PEMFC cathodes.

This study was supported by the US Department of Energy (DOE). Use of the Advanced Photon Source and the Electron Microscopy Center at Argonne was supported by DOE's Office of Science, under Contract DE-AC02-06CH11357. The authors wish to thank Drs D. Myers, X. Wang and N. E. Leyarovska for their helpful discussions and the experimental supports. The experimental support from the beamline 12-BM at the Advanced Photon Source is also gratefully acknowledged.

Notes and references

1 W. Vielstich, A. Lamm and H. Gasteiger, *Handbook of Fuel Cells: Fundamentals, Technology, Applications*, vol. 2: *Electrocatalysis*, John Wiley & Sons Inc., Chichester, UK, 2003.
2 R. Jasinski, *Nature*, 1964, **201**, 1212.
3 S. Lj. Gojković, S. Gupta and R. F. Savinell, *J. Electrochem. Soc.*, 1998, **145**, 3493.
4 M. Lefèvre, J. P. Dodelet and P. Bertrand, *J. Phys. Chem. B*, 2005, **109**, 16718.
5 M. Lefèvre, J. P. Dodelet and P. Bertrand, *J. Phys. Chem. B*, 2002, **106**, 8705.
6 F. Jaouen, S. Marcotte, J. P. Dodelet and G. Lindbergh, *J. Phys. Chem. B*, 2003, **107**, 1376.
7 M. Lefèvre and J. P. Dodelet, *Electrochim. Acta*, 2003, **48**, 2749.
8 P. H. Matter and U. S. Ozkan, *Catal. Lett.*, 2006, **109**, 115.
9 P. H. Matter, L. Zhang and U. S. Ozkan, *J. Catal.*, 2006, **239**, 83.
10 J. Yang and D.-J. Liu, *Carbon*, 2007, **45**, 2843.
11 R. Andrews, D. Jacques, A. M. Rao, F. Derbyshire, D. Qian, X. Fan, E. C. Dickey and J. Chen, *Chem. Phys. Lett.*, 1999, **303**, 467.
12 W. Q. Han, P. Kohler-Redlich, T. Seeger, F. Renst, M. Ruhle and N. Grobert, *Appl. Phys. Lett.*, 2000, **77**, 1807.
13 D. C. Koningsberger and R. Prins, *X-Ray Absorption: Principles, Applications, Techniques of EXAFS, SEXAFS and XANES*, John Wiley & Sons Inc., Chichester, UK, 1988.
14 C. Cartier, M. Momenteau, E. Dartyge, A. Fontaine, G. Tourillon, A. Michalowicz and M. Verdaguer, *J. Chem. Soc., Dalton Trans.*, 1992, **4**, 609.
15 M. C. Martins Alves, J. P. Dodelet, D. Guay, M. Ladouceur and G. Tourillon, *J. Phys. Chem.*, 1992, **96**, 10898.
16 S. Kim, T. Ohta and G. Kwag, *Bull. Korean Chem. Soc.*, 2000, **21**, 588.
17 S. Maldonado, S. Morin and K. J. Stevenson, *Carbon*, 2006, **44**, 1429.